

JAAS

Accepted Manuscript



This is an *Accepted Manuscript*, which has been through the Royal Society of Chemistry peer review process and has been accepted for publication.

Accepted Manuscripts are published online shortly after acceptance, before technical editing, formatting and proof reading. Using this free service, authors can make their results available to the community, in citable form, before we publish the edited article. We will replace this *Accepted Manuscript* with the edited and formatted *Advance Article* as soon as it is available.

You can find more information about *Accepted Manuscripts* in the [Information for Authors](#).

Please note that technical editing may introduce minor changes to the text and/or graphics, which may alter content. The journal's standard [Terms & Conditions](#) and the [Ethical guidelines](#) still apply. In no event shall the Royal Society of Chemistry be held responsible for any errors or omissions in this *Accepted Manuscript* or any consequences arising from the use of any information it contains.

The zircon 'matrix effect': evidence for an ablation rate control on the accuracy of U-Pb age determinations by LA-ICP-MS

Cite this: DOI: 10.1039/x0xx00000x

Received 00th January 2014,
Accepted 00th January 2014

DOI: 10.1039/x0xx00000x

www.rsc.org/

E. Marillo-Sialer,^a J. Woodhead,^a J. Hergt,^a A. Greig,^a M. Guillong,^b A. Gleadow,^a N. Evans,^c C. Paton^d

Many studies now acknowledge the occurrence of systematic discrepancies between U-Pb ages determined in zircons *in situ* by LA-ICP-MS and the benchmark analytical method ID-TIMS. In this study, we present detailed investigations into the ablation characteristics of zircons that suggest an underlying mechanism responsible for these age biases relative to ID-TIMS. Confocal laser scanning microscopy of laser ablation pits reveals that there are small but significant differences in the amount of material removed by the laser between different zircons. Based on numerous pit depth and LA-ICP-MS ²⁰⁶Pb/²³⁸U ratio measurements of a suite of natural zircon reference materials and samples, we demonstrate that a systematic age bias is strongly correlated with the offset in ablation rates between the primary reference material and sample zircons. We offer further insights concerning the effects of thermal annealing on the ablation behaviour of zircons and demonstrate that, although there is a change in laser ablation rates for annealed zircons, the variations between different zircons are not eliminated. Finally, we show that slight variations in laser focus also influence the ablation behaviour of zircons and may further degrade the accuracy of U-Pb age determinations.

Introduction

Matrix-matched external standardization is by far the most common approach used in U-Pb zircon geochronology by laser ablation inductively couple plasma mass spectrometry (LA-ICP-MS). The advantage of this approach is that it allows simultaneous correction for both mass bias and instrumental drift, as well as for laser induced elemental fractionation (LIEF) (also referred to as down-hole fractionation)¹, without the need for simultaneous TI-U (\pm Bi-Np) solution nebulization.²⁻⁴ The only limitation (and one common to most LA-ICP-MS U-Pb dating approaches) is that it necessarily requires that zircon reference materials and samples behave identically during the course of ablation.

Continuous advances in instrumentation and data handling schemes have promoted rapid improvements in the accuracy and reproducibility of U-Pb age determinations by LA-ICP-MS.^{5,6} Levels of accuracy and precision of 2-3% and 1% (2σ), respectively, are now commonly attributed to the technique.⁷ However, many individual laboratories have reported the occurrence of systematic bias in ²⁰⁶Pb/²³⁸U ages relative to corresponding ID-TIMS ages.⁸⁻¹¹

Klötzi, et al.⁹ further demonstrated the matrix-dependent nature of the observed bias. They note that, even after minimizing the effects of instrumental bias within a given analytical session, systematic shifts are still observed when using different primary zircon reference materials for age

calculation, and that in some cases these variations are well outside the estimated within-run precision.

Inter-laboratory comparison studies have also served to confirm the existence of apparent age biases in U-Pb zircon dating methods employing LA-ICP-MS.^{7, 12} In addition, these studies have highlighted the apparently random nature of the bias around the accepted ID-TIMS age of a zircon, with some laboratories reporting ages that are consistently too young and others reporting ages that are too old for the same zircon sample, even though the same primary reference material was used for calibration. As in Košler, et al.¹², the ²⁰⁶Pb/²³⁸U ages reported by individual laboratories are, in general, within $\pm 2\%$ of the ID-TIMS age. In several cases, however, the ages reported by different laboratories for the same zircon do not overlap within uncertainty budgets. Although the precision of age determinations suggests an underestimation of uncertainty related to the data reduction strategies employed by some laboratories, the variability in ablation conditions and zircon reference materials used for calibration are believed to be responsible for the range in offset observed in ²⁰⁶Pb/²³⁸U age determinations by LA-ICP-MS.

Differences in trace element composition⁸ between sample and reference zircons, as well as variations in the degree of radiation damage¹⁰, have been proposed to affect the laser beam-sample interaction and to cause fluctuations in the trend and degree of U-Pb laser induced elemental fractionation. Thus far, however, the nature of this matrix-related age bias remains

unconstrained due primarily to the lack of detailed fundamental studies on the interaction and response of natural zircons to laser radiation.

In this study we attempt to address some of these issues via a thorough examination of the morphology of individual ablation pits. Using detailed measurements of ablation pit depths, we demonstrate that systematic variations in laser penetration rate exist between different zircon matrices. Furthermore these differences translate into variations in the overall U-Pb fractionation behaviour observed during ablation.

In addition, we demonstrate how the final laser penetration rate in a zircon matrix may also be affected by inputs from non-matrix related sources, such as subtle variations in laser focus position. We attribute the apparent random nature of the $^{206}\text{Pb}/^{238}\text{U}$ age bias to a combination of matrix-related ablation behaviour and external factors affecting the absolute depth of the ablation pits.

Experimental

Samples

Six natural zircons previously characterised by ID-TIMS were employed in this study. These include the 91500¹³, Monastery¹⁴, Mud Tank¹⁵, Plešovice¹⁶, QGNG¹⁷ and Temora 2⁸ reference materials. The zircons were mounted in epoxy discs, polished to expose the grains then cleaned in ultrapure water and AR grade methanol prior to LA-ICP-MS analysis. All of these zircons are well-characterised and some are widely used as reference materials by the LA-ICP-MS U-Pb geochronology community. Their U-Pb ages range from ca. 90 Ma to 1852 Ma. A summary of relevant data for these samples is shown in Table 1.

Instrumentation

LA-ICP-MS. The majority of analyses were conducted at the University of Melbourne using a Laurin Technic HelEx ablation system constructed around a Compex 110, 193 nm ArF excimer laser (Lambda Physik, now Coherent USA) coupled to an Agilent 7700x quadrupole ICP-MS. The laser sampling system employs an imaging optics arrangement that provides uniform laser pulse energy across the surface area of the beam, resulting in the ablation of flat-bottomed pits with near vertical walls. Ablation occurs in a He atmosphere, and the ablation product is then rapidly combined with Ar gas before exiting the HelEx cell. A more detailed description of the laser instrumentation has been provided previously by Eggins, *et al.*¹ and Woodhead, *et al.*¹⁸.

Additionally, in order to test for consistency of results across ICP-MS instruments and laser ablation systems, we repeated some of the experiments using two other ns-pulse 193 nm ArF laser systems at ETH, Zurich, and Curtin University, Perth (see Table 2).

The three laser systems use a combination of Ar and He as carrier gas. They were operated at a repetition rate of 5 Hz, with a spot size of 30 – 33 μm . Energy densities were varied in the range of 1.5 – 3 J cm^{-2} depending on the design of the corresponding experiment. The acquisition parameters of the three ICP-MS systems were optimized before each analytical session to achieve high signal-to-noise ratio and low oxide production (ThO^+/Th^+ ratio of $\sim 0.2\%$). A summary of the instrumental parameters and operating conditions used for the LA-ICP-MS systems is listed in Table 2.

Confocal laser scanning microscopy. Accurate determination of laser pit dimensions, including diameter and depth, was achieved by means of a confocal laser scanning microscope (CLSM 700, Carl Zeiss). The CLSM allows the measurement of three-dimensional surface topography using optical sectioning. The confocal images were obtained by scanning through the z-axis of the ablation pits using a small pinhole corresponding to an optical slice of $\sim 0.4\ \mu\text{m}$, providing the vertical resolution of the method. The optical sections were then combined to build a three-dimensional image stack. Each CLSM analysis was performed over a $152\ \mu\text{m} \times 152\ \mu\text{m}$ area using a 50X objective, and a cut-off wavelength of 405 nm. In order to provide an unbiased representation of the 3D images, the variables of laser power, pinhole size and image detection were held constant throughout the study.

Analytical sequence and data reduction

Spot analyses of the various zircon reference materials were performed sequentially during each analytical session. A typical acquisition sequence consisted of a total of 8-10 spot analyses of each zircon sample, which were alternated in pairs. Either 91500 or Temora were used as primary reference material for age calculation. 2-3 spot analysis of the primary reference material were performed every 8-10 measurements of the zircon samples.

Typically 35 – 40 s of time-resolved data were acquired preceded by a 10 – 20 s background measurement. Corrections for instrumental drift, mass bias and LIEF, as well as U-Pb age calculations, relative to a zircon reference material were performed offline using the Iolite software package for data deconvolution and reduction. For detailed information on the functions and capabilities of Iolite and the built-in U-Pb data reduction scheme refer to Paton, *et al.*¹⁹ and Paton, *et al.*²⁰.

Table 1 Summary of relevant information for the zircon reference materials used in this study

| Zircon | Source | Pb $\mu\text{g g}^{-1}$ | U $\mu\text{g g}^{-1}$ | ID-TIMS age (Ma) | Reference |
|-----------|--|----------------------------|---------------------------|---------------------|---|
| 91500 | Pegmatite, Ontario, Canada | 16.3-19.3 | 67.7-87.7 | 1062.4 \pm 0.4 | Wiedenbeck, <i>et al.</i> ^{13, 21} |
| Monastery | Kimberlite, Free State, South Africa | < 3 | < 13 | 90.1 \pm 0.5 | Zartman, <i>et al.</i> ¹⁴ |
| Mud Tank | Carbonatite, Strangways Range, Northern Territory, Australia | 0.73-4.39 | 6.1-36.5 | 732 \pm 5 | Black and Gulson ¹⁵ |
| Plešovice | Perpotassic granulite, Bohemian Massif, Czech Republic | 21-158 | 465-3084 | 337.13 \pm 0.37 | Sláma, <i>et al.</i> ¹⁶ |
| QGNG | Gabbro, Cape Donington, South Australia | n.a. | 35-1151 | 1842 \pm 3.1 | Black, <i>et al.</i> ¹⁷ |
| Temora 2 | Gabbroic diorite, New South Wales, Australia | n.a. | 82-320 | 416.78 \pm 0.33 | Black, <i>et al.</i> ⁸ |

Table 2 Operating parameters for the LA-ICP-MS systems used for the experiments

| | LA-ICP-MS | | |
|---|---|--|---|
| Laboratory name | School of Earth Sciences, University of Melbourne, Melbourne Australia | Department of Earth Sciences, ETH Zurich, Zurich, Switzerland | John de Laeter Centre, Curtin University, Perth, Australia |
| Laser | Compex 110, Coherent | CompexPro 102, Coherent | CompexPro 102, Coherent |
| Wavelength | 193 nm | 193 nm | 193 nm |
| Pulse width | 25 ns | 25 ns | 25 ns |
| Energy density | 2 – 2.5 J cm ⁻² | 1.5 – 3 J cm ⁻² | 2 – 2.7 J cm ⁻² |
| Repetition rate | 5 Hz | 5 Hz | 5 Hz |
| Spot size | 32 μm | 30 μm | 33 μm |
| Ablation cell | Laurin Technic HelEx | Laurin Technic S155 | Laurin Technic M50 |
| Effective cell volume | ~2 cm ³ | ~1 cm ³ | ~1 cm ³ |
| He gas flow | 0.3 L min ⁻¹ | 0.7 L min ⁻¹ | 0.68 L min ⁻¹ |
| ICP-MS | Agilent 7700x | Thermo Element XR | Agilent 7700x |
| RF power | 1300 W | 1450 W | 1360 W |
| Ar gas flow | 0.98 – 1 L min ⁻¹ | 0.995 L min ⁻¹ | 0.98 L min ⁻¹ |
| N₂ gas flow | – | 1 mL min ⁻¹ | 2.8 mL min ⁻¹ |
| Masses measured | ²⁹ Si, ³¹ P, ⁴⁹ Ti, ⁸⁹ Y, ⁹¹ Zr, ¹³⁹ La, ¹⁴⁰ Ce, ¹⁴⁶ Nd, ¹⁴⁷ Sm, ¹⁵³ Eu, ¹⁶³ Dy, ¹⁷² Yb, ¹⁷⁵ Lu, ¹⁷⁸ Hf, ²⁰⁶ Pb, ²⁰⁷ Pb, ²⁰⁸ Pb, ²³² Th, ²³⁸ U | ²⁰² Hg, ²⁰⁴ Pb, ²⁰⁶ Pb, ²⁰⁷ Pb, ²⁰⁸ Pb, ²³² Th, ²³⁵ U, ²³⁸ U | ²⁹ Si, ⁴⁹ Ti, ⁹¹ Zr, ¹⁷⁸ Hf, ²⁰² Hg, ²⁰⁴ Pb, ²⁰⁶ Pb, ²⁰⁷ Pb, ²⁰⁸ Pb, ²³² Th, ²³⁵ U, ²³⁸ U |
| ²⁴⁸ThO/²³²Th | <0.2% | <0.2% | 0.18% |

Background subtracted ²⁰⁶Pb/²³⁸U signal ratios were inspected closely for any problems related to common Pb surface contamination and sample heterogeneity. Where required LIEF was modelled using an exponential function as described by Paton, *et al.*¹⁹

Results and discussion

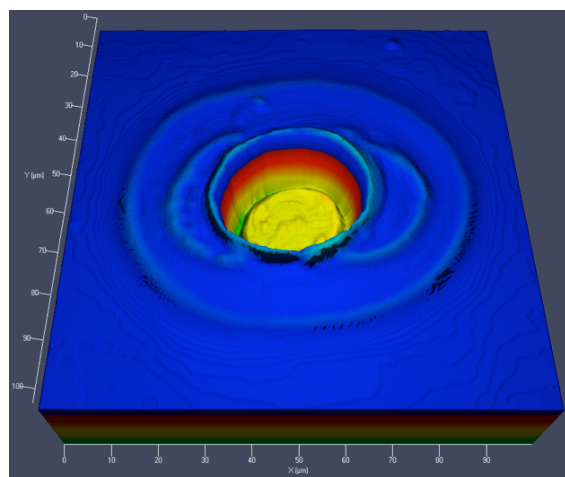
Ablation behaviour of zircons

Pit morphology. The morphology of the ablation pits formed after repetitive laser pulses provides a way to evaluate the ablation mechanism involved.²² Fig. 1A shows the three-dimensional topographic image of a typical ablation pit produced in zircon. The pit was generated by firing 150 pulses at ~2 J cm⁻². The morphology of all the ablation pits obtained shows some evidence of small wavelike structures on the bottom surface, which is indicative of localized melting caused by the thermal contribution to the ablation.²³ However, neither significant surface roughness nor indications of droplet-like macro particulates were detected at the laser energy densities tested, suggesting an efficient thermal propagation process without explosive boiling of the target zircon.²⁴ The deposit or blanket that is visible on the surface surrounding the ablation pit in Fig. 1A consists of nanometre scale particles that condensed out of the ablation plume, as shown by Eggs, *et al.*¹ and Woodhead, *et al.*¹⁸

Depth measurements. Cross-sectional profiles of ablation craters were obtained within the LSM 700 Zen 2010 interface software (Carl Zeiss, Germany) of the CSLM by drawing a profile line across the centre of each pit (Fig. 1B). Pit depth and diameter were measured from the crater profile, and ablation rates were estimated by averaging the depth per laser pulse of several ablation craters. Clear differences in ablation rate were observed for various zircons ablated under identical experimental conditions (Fig. 2).

The design of the analytical sequence, with repeated ‘cycling’ through the various zircons, eliminates any differences in ablation rate caused by slight temporal

(A)



(B)

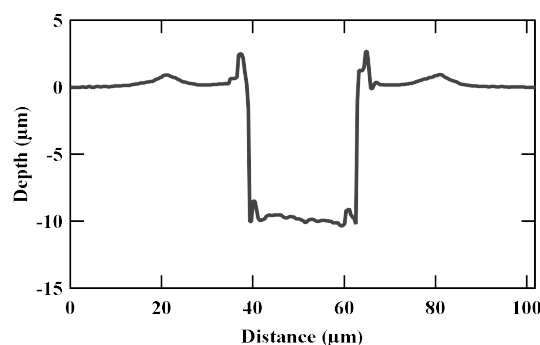


Fig. 1 (A) Representative 3D topographic view and (B) cross-section profile of an ablation pit obtained after ablation of a zircon natural sample using a 193 nm ArF excimer laser and 150 laser pulses at ~2 J cm⁻², with exaggerated scale on y-axis. Note the ‘top-hat’ profile and relatively flat bottom of the ablation pit. The condensate deposits surrounding the ablation pit show no evidence of larger-scale droplets characteristic of an explosive ablation.

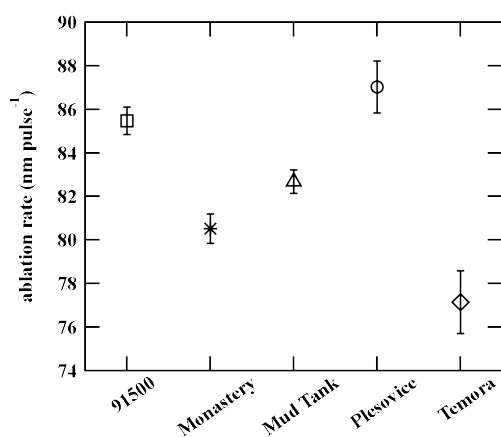


Fig. 2 Ablation rate in zircons obtained during a single analytical session by ablating with 300 laser pulses at $\sim 2 \text{ J cm}^{-2}$ at the University of Melbourne. Pit depths were measured by means of confocal laser scanning microscope. Error bars represent 2 s.e. of the measurements on several different spots.

fluctuations in instrumental parameters. Consequently, we believe that the differences in ablation rate between zircons reported here are not associated with temporal changes in parameters known to have an effect on the mass removal, such as energy density, pulse length of the laser beam and laser focus.²⁵⁻²⁷

The differences in ablation behaviour are instead likely to be related to the intrinsic characteristics of the material ablated, i.e. the zircon matrix. Slight variations in optical and thermo-physical properties between zircons due to, for example, radiation damage-induced lattice defects, will affect the laser-zircon interaction, and thus the amount of material removed by each laser pulse.

Vermeesch, *et al.*²⁸ have previously reported variations in the depth of pits ablated in three different zircons using a Nd-YAG laser operated at 213 nm, 8 Hz and $\sim 2 \text{ J cm}^{-2}$. The differences in pit depth ranged from 0.72 to 2 μm , in good agreement with our observations. Nevertheless, little is known regarding the extent to which this variability identified in ablation behaviour between zircons affects the measurement of $^{206}\text{Pb}/^{238}\text{U}$ signal ratios observed during LA-ICP-MS.

The effect of zircon ablation behaviour on U-Pb ratios and resulting U-Pb ages

Table 3 Ablation rates for the Temora zircon at varied laser energy densities and associated $^{206}\text{Pb}/^{238}\text{U}$ ages calculated using (*) as the reference zircon, and others as 'unknowns'. Extended data table is provided in the Electronic Supplementary Information (ESI Table 1).

| Energy density (J cm^{-2}) | Age (Ma) | | | | Ablation behaviour | | | |
|---------------------------------------|----------------------------------|--------------------|--|---------------------|--------------------------|-------------------|---|-------------------|
| | $^{206}\text{Pb}/^{238}\text{U}$ | $\pm 2\text{s.e.}$ | $\Delta^{206}\text{Pb}/^{238}\text{U}$ Age % | $\pm \text{s.e.}^a$ | Ablation rate (nm/pulse) | $\pm \text{s.e.}$ | $\Delta \text{AR}_{(\text{Smp-RM})} \%$ | $\pm \text{s.e.}$ |
| 1.56 | 405.68 | 0.84 | -2.7% | 0.3% | 54.5 | 0.2 | -25.3% | 0.7% |
| 1.80 | 413.7 | 2.5 | -0.7% | 0.7% | 65.3 | 0.2 | -10.4% | 0.7% |
| 2.08* | 416.2 | 1.9 | -0.1% | 0.5% | 73.0 | 0.3 | +0.0% | 0.0% |
| 2.32 | 421.6 | 2.1 | +1.2% | 0.6% | 81.5 | 0.9 | +11.8% | 1.6% |
| 2.61 | 427.4 | 2.6 | +2.5% | 0.7% | 88.0 | 0.5 | +20.6% | 1.0% |
| 2.84 | 431.2 | 1.6 | +3.5% | 0.5% | 94.8 | 0.8 | +29.9% | 1.4% |

The quoted standard errors (s.e.) represent the precision on an individual analysis and not the full external reproducibility of the U-Pb method.

^aPropagated to include the standard error of the TIMS $^{206}\text{Pb}/^{238}\text{U}$ age for the Temora zircon.

As a first demonstration, we have used the Temora zircon reference material to evaluate the effect of variations in ablation rate on the measured $^{206}\text{Pb}/^{238}\text{U}$ ratios. First, we conducted a series of single spot ablations using 200 laser pulses and six different energy densities during a single analytical session at ETH Zurich. Only a slight variation in energy density was required to simulate the range of laser penetration rates for the different zircons we observed previously (Fig. 2), but in this case using just the Temora zircon.

The energy density values used, as well as the ablation rates achieved, are shown in Table 3. The slight increase in penetration depth, on the order of 1 – 2 μm for 200 pulses, produces a change in the $^{206}\text{Pb}/^{238}\text{U}$ fractionation trend with time and a systematic shift in the recorded $^{206}\text{Pb}/^{238}\text{U}$ ratios to higher values on the order of 1-2%, as shown in Fig. 3. Visual analysis of the morphology of the ablation pits showed no evidence of change in ablation mechanism for the energy densities used, therefore the observed variations in $^{206}\text{Pb}/^{238}\text{U}$ ratio are attributed solely to the rate at which material is removed during pulsed laser sampling.

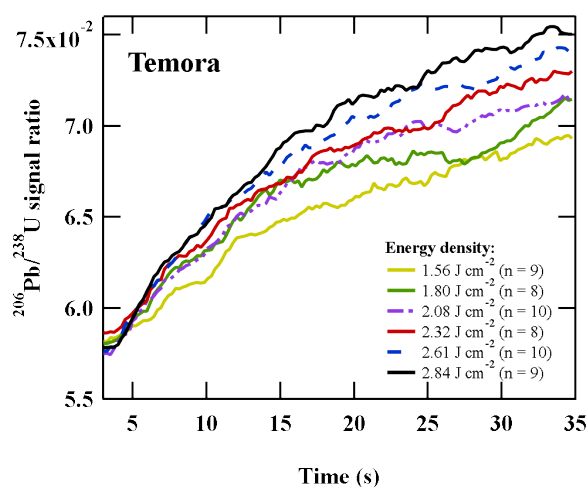


Fig. 3 Variation in down-hole elemental fractionation with laser energy density. The $^{206}\text{Pb}/^{238}\text{U}$ ratios are baseline-subtracted and mass bias corrected. The plot illustrates the ratios before the down-hole correction was applied in order to show the down-hole fractionation patterns. A slight increase in laser fluence produces a subtle increase in the amount of mass removed per laser pulse, and a significant increase in $^{206}\text{Pb}/^{238}\text{U}$ ratio measured by the LA-ICP-MS.

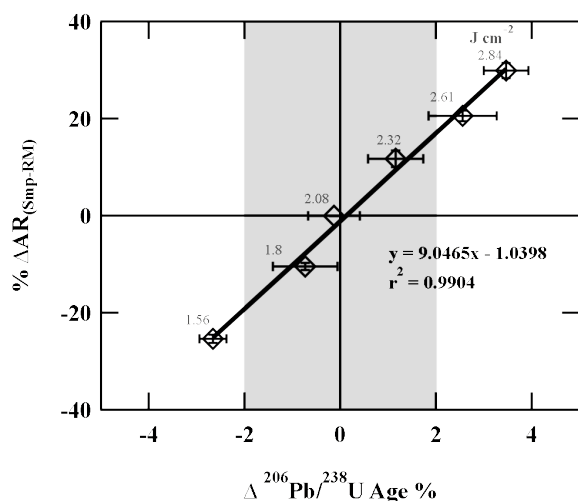


Fig. 4 Ablation rate percent offset versus $^{206}\text{Pb}/^{238}\text{U}$ age percent offset (data from Table 3). The experiment was performed at ETH Zurich. The Temora zircon was ablated using different energy densities in order to achieve slightly different ablation rates, and thus study the effect of ablation rate on calculated $^{206}\text{Pb}/^{238}\text{U}$ ages. Ablation rate offset is calculated relative to the ablation rate of the zircon used as reference for age calculation (Temora ablated at a laser fluence of 2.08 J cm^{-2}). Age offset is calculated for the measured $^{206}\text{Pb}/^{238}\text{U}$ age relative to the accepted ID-TIMS age. Error bars represent 2 s.e. For reference, the shaded area represents $\pm 2\%$ $^{206}\text{Pb}/^{238}\text{U}$ age uncertainty.

In order to demonstrate the potential of such small effects to influence U-Pb ages, the $^{206}\text{Pb}/^{238}\text{U}$ ages were calculated based on the downhole-corrected $^{206}\text{Pb}/^{238}\text{U}$ ratio obtained for each energy density tested and using the $^{206}\text{Pb}/^{238}\text{U}$ ratio from the Temora zircon ablated at 2.08 J cm^{-2} as the reference value for calibration (Table 3).

Considering the effects of subtle changes in laser penetration rate on the measured $^{206}\text{Pb}/^{238}\text{U}$ ratio noted above, it is reasonable to infer that any systematic bias in the calculated $^{206}\text{Pb}/^{238}\text{U}$ age, relative to the accepted ID-TIMS age, would correlate to the offset in amount of material removed between the 'reference' and 'sample' experiments. Thus we calculate the accuracy of $^{206}\text{Pb}/^{238}\text{U}$ age determinations, expressed as percent offset from the accepted ID-TIMS as follows

$$\Delta \frac{^{206}\text{Pb}}{^{238}\text{U}} \text{ Age } \% = \frac{\left(\frac{^{206}\text{Pb}}{^{238}\text{U}} \text{ Age}\right)_{\text{meas}} - \left(\frac{^{206}\text{Pb}}{^{238}\text{U}} \text{ Age}\right)_{\text{TIMS}}}{\left(\frac{^{206}\text{Pb}}{^{238}\text{U}} \text{ Age}\right)_{\text{TIMS}}} \times 10^2$$

for the Temora zircons ablated using different laser drill rates, and plot these against the corresponding ablation rate offset ($\Delta \text{AR}_{(\text{Smp-RM})}$) of the form

$$\Delta \text{AR}_{(\text{Smp-RM})} \% = \frac{\text{AR}_{\text{Smp}} - \text{AR}_{\text{RM}}}{\text{AR}_{\text{RM}}} \times 10^2$$

where AR_{RM} is the ablation rate of the zircon used for calibration and AR_{Smp} the ablation rate for the zircon sample (Fig. 4). As seen in Fig. 4, there is a striking positive correlation ($r^2 = 0.99$) between the calculated age offset and the offset in ablation rates. This suggests that subtle differences in the rate of sample removal between reference material and sample can have significant effects on calculated ages. In this experiment, a range of variation in $^{206}\text{Pb}/^{238}\text{U}$ age offset from 0.7% to 3.5%

was obtained for differences in ablation rate of the order of 10.4% to 30%, which correspond to ablation pit depth differences of only $1.5 \mu\text{m}$ to $4.4 \mu\text{m}$. Importantly, these variations in drill rate have approximately the same order of magnitude as those detected between different zircon reference materials in the first part of our study (Fig. 2).

Furthermore, the extent of $^{206}\text{Pb}/^{238}\text{U}$ age variation is comparable to the degree of systematic bias in calculated $^{206}\text{Pb}/^{238}\text{U}$ ages that is usually ascribed to so-called 'matrix-effects' by the U-Pb LA-ICP-MS geochronology community, suggesting that differences in ablation rate between zircons may account entirely for this matrix-related age bias. To further explore this premise, we extended our analysis to the results of $^{206}\text{Pb}/^{238}\text{U}$ age determinations obtained for different zircon reference materials during three analytical sessions at the University of Melbourne over a period of three months. The 91500 zircon was the primary calibrant for all these age calculations. The results are summarised in Fig. 5. As expected from our previous experiments, a higher laser penetration depth for the zircon sample, compared to that of the zircon reference, leads to an increase in its measured $^{206}\text{Pb}/^{238}\text{U}$ ratio and thus, to an overestimation of the corresponding age. The opposite is also true, i.e. if the ablation rate of the sample is lower than that of the reference, the elemental bias correction factor calculated using the accepted $^{206}\text{Pb}/^{238}\text{U}$ ratio of the zircon reference is too high, resulting in an underestimation of the calculated $^{206}\text{Pb}/^{238}\text{U}$ age for the zircon sample. It is also worth nothing in this context that the use of a different down-hole correction protocol (e.g. linear fit) would not affect the $^{206}\text{Pb}/^{238}\text{U}$ age bias results obtained in this experiment.

This is a highly significant observation which reveals that ablation rates alone may help to explain the systematic age biases ('matrix effects') often observed when using different zircons as reference materials. As previous studies have shown,

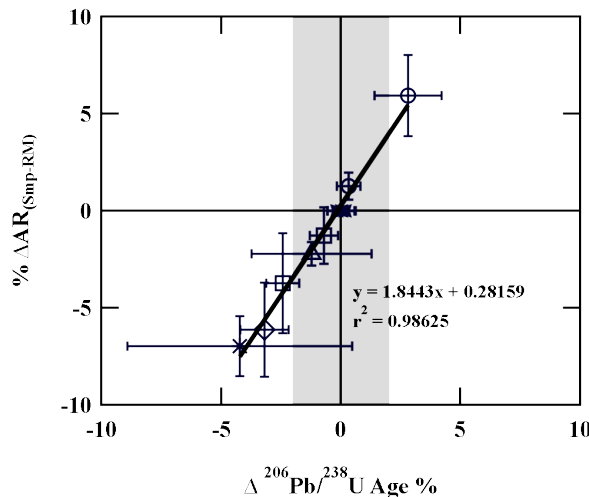


Fig. 5 Variations in $\Delta^{206}\text{Pb}/^{238}\text{U}$ % Age with % ablation rate offset for (○) Plešovice, (□) 91500, (◇) Temora, (△) Mud Tank, (★) Monastery. Ablation rate offset is calculated relative to the 91500 zircon. Data are from three separate analytical sessions performed over a period of three months at the University of Melbourne. Error bars represent 2 s.e. Counting statistics are the dominant source of error in the age offset estimations for the Mud Tank and Monastery zircons due to very low ^{238}U and ^{206}Pb abundances. The systematic shift observed between the calculated ages is related to the difference in ablation behaviour, i.e. amount of mass removed per laser pulse, between the zircon reference (91500) and sample. For reference, the shaded area represents $\pm 2\%$ $^{206}\text{Pb}/^{238}\text{U}$ age uncertainty.

there is a close relationship between increasing LIEF and increasing depth of the pit. A number of different mechanisms have been proposed to underlie the down-hole fractionation process, including (i) preferential volatilization of more volatile elements (e.g. Pb) from the fluid phase or melt formed in the ablation pit and its surroundings, leading to enrichment of refractory elements (e.g. U) as the ablation pit deepens²⁹; (ii) preferential condensation of the ablated vapour onto the walls of the ablation crater, with refractory phases condensing earlier than volatile phases. The portion of refractory phase that condenses is suggested to increase as ablation proceeds due to increase in sidewall area^{1, 30}; and (iii) for crystalline samples, the formation of different phases caused by thermal decomposition (e.g. zircon to baddeleyite and quartz), and the subsequent redistribution of elements within these phases by geochemical affinity. The rate of phase formation in zircon is related to the surface area affected by thermal propagation of the laser beam, and thus increases with sidewall area of the pit³¹.

Given these findings it is now important to understand the underlying causes of variability in ablation behaviour between different zircons.

Variables that affect the ablation behaviour of zircons

One important observation in reading the extensive literature on laser ablation U/Pb geochronology is that the ²⁰⁶Pb/²³⁸U age biases observed across the LA-ICP-MS geochronology community¹² appear to have a random component. This suggests that the sources of variability in ablation behaviour are likely to be associated with variables that might change over the course of an analytical run and from day-to-day fluctuations.

Matrix effects. Variations in laser removal rate due to subtle differences in the degree to which zircons absorb laser radiation are associated with the optical and mechanical character of the zircon matrix. The optical and physical properties of zircons vary depending on their crystalline state, which is at the same time controlled by the presence of lattice defects caused by both radiation damage and the substitution of certain trace elements within the zircon structure.³²⁻³⁴ Crystallographic orientation may also contribute to variation in ablation rates particularly for anisotropic minerals such as zircon samples, since different crystallographic planes exhibit differences in optical absorption.³⁵

Attempts to identify the causes of the systematic bias in zircon LA-ICP-MS ²⁰⁶Pb/²³⁸U dating have so far considered only single sources of variation.^{8, 10, 36} A linear correlation analysis was undertaken to investigate the relationship between measured ablation rate and single trace element abundances for the data set obtained at the University of Melbourne and reveals no apparent correlation between these variables. Similar results were obtained for a correlation analysis between ablation rates of the zircons studied and their total self-irradiated alpha-doses (calculated from U and Th concentrations and U-Pb age as in Nasdala, *et al.*³⁷). It is therefore likely that the development of a proxy capable of providing an adequate characterization of the ablation behaviour of a specific zircon matrix will require the incorporation of multiple components.

Although a comprehensive assessment of likely sources of matrix effects is beyond the scope of this contribution, the influence of radiation damage is examined below. In their recent detailed study, Allen and Campbell¹⁰ addressed the zircon matrix-related age bias and provided strong support for the role of radiation damage in the observed systematic shifts in

LA-ICP-MS U-Pb ages. To investigate this issue further we have studied the effect of annealing on the ablation behaviour of zircons. Several grains of the Temora, Plešovice and QGNG zircons were annealed in air at 850 °C for 48 h. The annealed zircons were mounted in a single epoxy disc along with unprocessed examples of the same zircons, polished and cleaned using standard procedures. All the zircon samples (annealed and unprocessed) were ablated using 150 laser pulses at ~2 J cm⁻². The depth of each resultant ablation pit was measured by CLSM. Pit depth values were used to calculate the laser ablation rate into each zircon sample (Fig. 6).

Three important observations are evident from the results. First, there are clear and significant differences between the laser penetration rates of annealed and natural grains of the same reference zircons. In the case of the annealed zircons, a lower ablation rate is produced compared to that of the corresponding natural sample. Ablation rates for the Temora, Plešovice and QGNG zircons decreased by 5.6%, 5.2% and 4.2% after annealing, respectively. This decrease can be explained by the increase in crystal density due to reconstitution of the crystal structure through thermal annealing. A second observation is that, consistent with the results displayed in Fig. 2, there are different laser penetration rates between the various reference zircons. The third observation, however, is perhaps the most remarkable and unexpected; that is, the differences in ablation rates between reference zircons appear to be maintained even after annealing. Thus despite a universal reduction in ablation rate with annealing, the fact that the observed decrease is approximately equal for the three zircon samples strongly suggests that any systematic bias in the measured LA-ICP-MS ²⁰⁶Pb/²³⁸U ages, relative to the corresponding ID-TIMS age, will still be present after annealing.

In order to verify the above statement, we calculated the ²⁰⁶Pb/²³⁸U ages for annealed and untreated zircons using Temora (untreated) as reference material; results are shown in

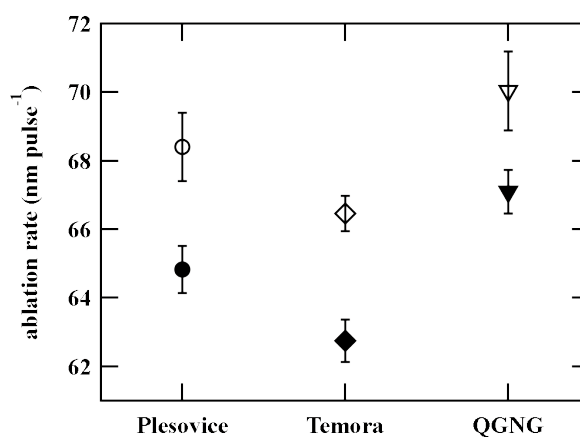


Fig. 6 Ablation rates measured for the Plešovice, Temora and QGNG zircons. Solid shapes correspond to zircons that were annealed at 850 °C for 48 h. Error bars represent 2 s.e. of multiple measurements. Annealed and natural zircons were ablated during the same analytical session by firing 150 laser pulses at ~2 J cm⁻². There is a systematic trend towards lower ablation rates for annealed samples that agrees with the increase in crystal density due to annealing. Note, however, that the differences in ablation rate between zircon matrices are maintained even after annealing.

Table 4 $^{206}\text{Pb}/^{238}\text{U}$ ages for annealed and natural zircons calculated using Temora as the reference zircon

| zircon | n | $^{206}\text{Pb}/^{238}\text{U}$ Age (Ma) | ± | 2 s.e. |
|-----------------|----------------|---|---|--------|
| <i>natural</i> | | | | |
| Temora | 10 | 416.2 | ± | 1.3 |
| Plešovice | 9 ^a | 338.08 | ± | 0.85 |
| QNGG | 9 ^a | 1866.1 | ± | 7.1 |
| <i>annealed</i> | | | | |
| Temora | 10 | 412.9 | ± | 3.4 |
| Plešovice | 10 | 335.7 | ± | 2.3 |
| QNGG | 10 | 1843.3 | ± | 6.4 |

Standard errors (s.e.) represent the precision on an individual analysis.
^aOne spot analysis rejected. Rejection based on 2-sigma outlier rejection.

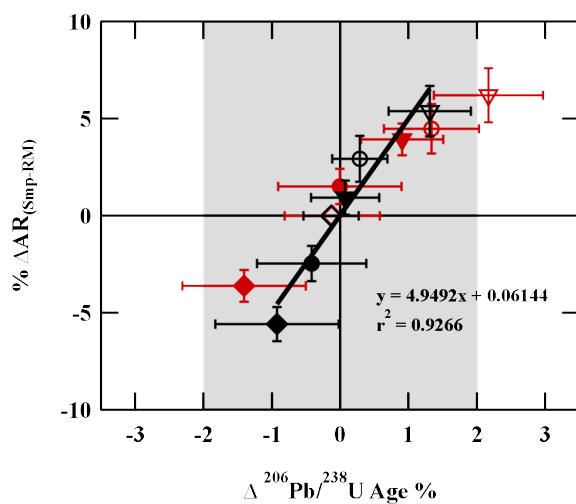


Fig. 7 Ablation rate per cent offset vs $^{206}\text{Pb}/^{238}\text{U}$ age per cent offset for (\diamond) Temora, (\circ) Plešovice and (∇) QNGG zircons. Data from an analytical session performed at the University of Melbourne (black) and at Curtin University (red). Solid shapes correspond to zircons that were annealed before LA-ICP-MS analysis: (\blacklozenge) Temora, (\bullet) Plešovice, (\blacktriangledown) QNGG. Ablation rate offsets were calculated relative to the ablation rate for the zircon standard Temora (\diamond). Error bars are 2 s.e. For reference, the shaded area represents $\pm 2\%$ $^{206}\text{Pb}/^{238}\text{U}$ age uncertainty.

Table 4. It is clear that systematically younger ages are obtained for the annealed zircons, which is in agreement with the ablation rate hypothesis (Fig. 6). The correlation between ablation behaviour and $^{206}\text{Pb}/^{238}\text{U}$ age offset is shown in Fig. 7. The positive linear trend in age offset with amount of material removed during laser sampling remains significant ($r^2 = 0.93$) for annealed and untreated zircons. Thus, we conclude that there is no change in the mechanism controlling the fractionation of $^{206}\text{Pb}/^{238}\text{U}$ ratio for annealed zircons.

In order to rule out any laboratory-specific effects, we repeated the analysis using a laser ablation system at Curtin University, Perth, Western Australia. The results are shown in red symbols in Fig. 7 and are very similar to those obtained at The University of Melbourne Fig. 7 (black). The small laboratory-to-laboratory differences in ablation rates can be explained by a slightly different laser focus between the laser ablation systems. While the availability of a confocal scanning laser microscope at the University of Melbourne allowed us to refine this focus so that it is located at the exact sample surface

level, this improved laser focus calibration was not possible for the other laser ablation systems tested.

These experimental results suggest that, although annealing has a marked effect on the ablation behaviour of zircons, it does not necessarily improve the accuracy of the $^{206}\text{Pb}/^{238}\text{U}$ ages obtained by LA-ICP-MS relative to their corresponding ID-TIMS ages, in contrast to the findings of Allen and Campbell¹⁰.

Laser focal plane. In the course of our studies, it has also become apparent that there are other potential influences on ablation rates that are not entirely explained by the zircon matrix. Our experimental observations showed a clear spatial component to some variations, as they were evident in cases where the zircon reference and samples were mounted in separate discs of epoxy and placed in different positions across the ablation cell.

After consideration of the several possible external components that may affect the laser ablation process, we established that the detected residual variations could be attributed to slight changes in the distance between the laser beam focal plane and the target surface. Liu, *et al.*²⁷ reported the effect of different laser focusing conditions on the $^{206}\text{Pb}/^{238}\text{U}$ ratio measured in NIST 610 glass. They showed that substantial changes in ablation pit dimensions occurred by altering the position of the laser focus by 1-1.5 mm relative to the laser surface, which in turn caused significant variations in the measured $^{206}\text{Pb}/^{238}\text{U}$ signal ratio for the glass sample. Here, we show that even with 'top-hat' shaped beam profiles, much smaller changes in laser focus position can produce significant variation in the ablation behaviour of zircons.

Ablation of the Plešovice zircon using different focus positions was performed at ETH Zurich. Changes in the distance between the focal plane and the sample surface were achieved by gradually varying the position of the projection lens in the z-axis. The pits were ablated at each focus position using 205 laser pulses at $\sim 2 \text{ J cm}^{-2}$ during a single analytical session. Fig. 8(A) shows the topographic view of representative pits obtained at three different focus positions. These gradual changes (of the order of tens of microns) produced no obvious modifications in shape and diameter of the resultant ablation pits using conventional optical inspection, and thus would not be obvious to the general user. Subtle differences in shape and size can be measured only after analysis by CLSM and significant changes to the ablation pit profile are observed at distances from the focal plane of $\geq 30 \mu\text{m}$. Measured ablation rates are illustrated in Fig. 8(B) as a function of the distance between focal plane and focus position. It can be observed that small but significant changes in laser penetration depth, up to $\sim 4.1\%$, are obtained by ablating at a subtly different laser focus position ($\leq 30 \mu\text{m}$).

Based on previous observations, an age bias of up to $\sim 1.5\%$ can be expected if the surface of the reference and sample zircons are not aligned to the same plane, but differ by $\leq 30 \mu\text{m}$. During a typical analytical session such variations may derive from a variety of factors. These may include (but are not limited to) epoxy mounts where zircons, reference or sample, protrude to a certain extent above the epoxy disc surface due to over polishing, misalignments in the sample holder, or inaccuracies in focus at the start of the session. Subtle differences such as these can easily go unnoticed by the LA-ICP-MS user, and may contribute to the apparently random character of the systematic bias in measured $^{206}\text{Pb}/^{238}\text{U}$ ages across the zircon LA-ICP-MS geochronology community. Clearly precise sample preparation methodologies are a critical

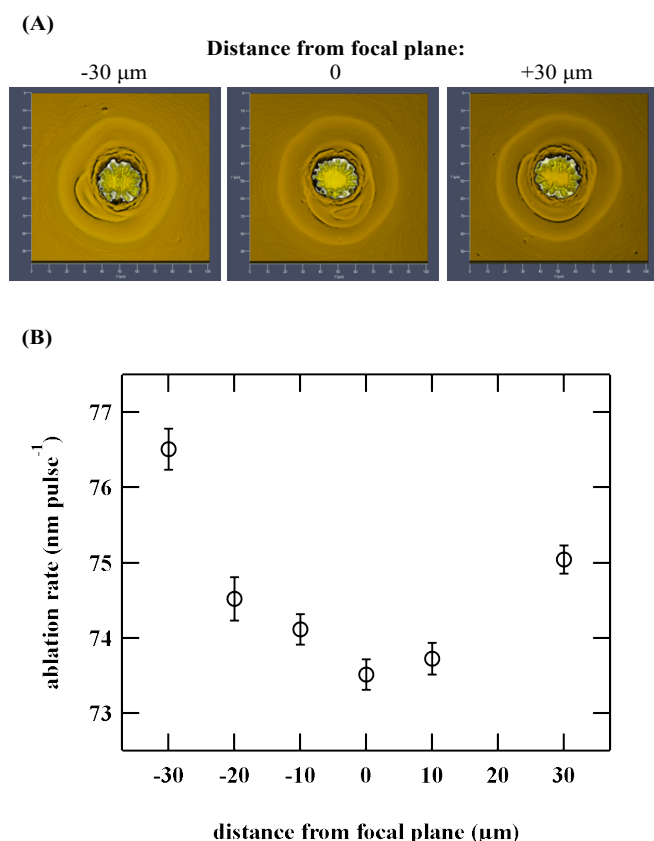


Fig. 8 (A) Topographic view of laser ablation pits measured using confocal laser scanning microscopy. The pits were produced after ~200 laser pulses at $\sim 2 \text{ J cm}^{-2}$ at different focus positions. Note the slight increase in surface roughness at the bottom of the pit at $30 \mu\text{m}$ below the focal point. (B) Ablation rates measured for pits ablated at different focus positions during a single analytical session. All the other ablation parameters were kept constant.

component of achieving high accuracy results. We also note that some laser optic designs, particularly those with high numerical aperture and hence shallow depth of field (e.g. Schwarzschild lens), although providing some benefits, will likely exacerbate issues requiring precise laser focus such as those discussed in this contribution.

Conclusions

The results presented in this paper suggest that the observed biases in LA-ICP-MS zircon $^{206}\text{Pb}/^{238}\text{U}$ ages, relative to the ID-TIMS reference ages, can be entirely explained by the differences in ablation rate between reference and sample zircons.

Both the intrinsic optical properties of the zircon matrix itself and subtle defocusing effects of the laser beam lead to variations in zircon ablation rates which can, on a day-to-day or lab-to-lab basis, give the impression of being almost random in nature, despite an underlying control. We also conclude that, although radiation damage plays a major role in defining the optical and mechanical character of zircons, annealing of zircons in itself does not completely eliminate the differences in ablation behaviour between different zircon matrices and thus is of limited value in improving the accuracy of LA-ICP-MS zircon dating.

In future, the ability to precisely measure laser penetration depths in a variety of zircons will enable us to quantify the LA-ICP-MS $^{206}\text{Pb}/^{238}\text{U}$ age bias. Based on this knowledge, it is hoped that it will be possible to develop a proxy able to accurately predict differences in ablation rates between zircons and that this could provide a new strategy for improvement of the accuracy of $^{206}\text{Pb}/^{238}\text{U}$ age determinations in zircons by LA-ICP-MS.

Acknowledgements

E. M-S gratefully acknowledges a University of Melbourne research scholarship. Mike Shelley is thanked for technical advice and for assistance with laser energy density measurements. The comments of two anonymous referees helped to improve the quality of this manuscript.

Notes

^a School of Earth Sciences, The University of Melbourne, Parkville, Vic 3010, Australia.

^b Department of Earth Sciences, ETH Zurich, 8092 Zurich, Switzerland.

^c AuScope GeoHistory Facility, John de Laeter Centre for Isotope Research, Curtin University, Perth, WA 6845, Australia.

^d Centre for Star and Planet Formation, Natural History Museum of Denmark, University of Copenhagen, Copenhagen DK-1350, Denmark.

† Electronic Supplementary Information (ESI) available: Results of individual spot analyses. See DOI: 10.1039/b000000x/

References

- S. Eggins, L. Kinsley and J. Shelley, *Applied Surface Science* 1998, **278**.
- I. Horn, R. Rudnick and W. McDonough, *Chemical Geology*, 2000, **167**, 405.
- J. Košler, H. Fonneland, P. Sylvester, M. Tubrett and R. Pedersen, *Chemical Geology*, 2002, **182**, 605.
- R. Cox, D. Wilton and J. Košler, *The Canadian Mineralogist*, 2003, **41**, 273.
- A. Cocherie and M. Robert, *Gondwana Research*, 2008, **14**, 597.
- M. Wiedenbeck, R. Bugoi, M. J. M. Duke, T. Dunai, J. Enzweiler, M. Horan, K. Jochum, K. Linge, J. Košler, S. Merchel, L. Morales, L. Nasdala, R. Stalder, P. Sylvester, U. Weis and A. Zoubir, *Geostandards and Geoanalytical Research*, 2012, **36**.
- J. Hanchar, in *Eos Trans. AGU, Fall Meet. Suppl.* 2009, vol. 90, Abstract V53B-04.
- L. Black, S. Kamo, C. Allen, D. Davis, J. Aleinikoff, J. Valley, R. Mundil, I. Campbell, R. Korsch, I. Williams and C. Foudoulis, *Chemical Geology*, 2004, **205**, 115.
- U. Klötzli, E. Klötzli, Z. Günes and J. Košler, *Geostandards and Geoanalytical Research*, 2009, **33**, 5.
- C. Allen and I. Campbell, *Chemical Geology*, 2012, **332-333**, 157.
- G. Gehrels, V. Valencia and J. Ruiz, *Geochemistry Geophysics Geosystems*, 2008, **9**, 1.
- J. Košler, J. Sláma, E. Belousova, F. Corfu, G. Gehrels, A. Gerdes, M. Horstwood, K. Sircombe, P. Sylvester, M. Tiepolo, M. Whitehouse and J. Woodhead, *Geostandards and Geoanalytical Research*, 2013, **37**, 243.
- M. Wiedenbeck, P. Allé, F. Corfu, W. L. Griffin, M. Meier, F. Oberli, A. V. Quadt, J. C. Roddick and W. Spiegel, *Geostandards Newsletter*, 1995, **19**, 1.
- R. Zartman, S. Richardson, J. Gurney and R. Moore, 7th International Kimberlite Conference, Cape Town, South Africa, 1998.
- L. Black and B. Gulson, *BMR Journal of Australian Geology and Geophysics*, 1978, **3**, 227.
- J. Sláma, J. Košler, D. J. Condon, J. L. Crowley, A. Gerdes, J. M. Hanchar, M. S. A. Horstwood, G. A. Morris, L. Nasdala, N.

- 1 Norberg, U. Schaltegger, B. Schoene, M. N. Tubrett and M. J. Whitehouse, *Chemical Geology*, 2008, **249**, 1.
- 2
- 3 17 L. Black, S. Kamo, C. Allen, J. Aleinikoff, D. Davis, R. Korsch and C. Foudoulis, *Chemical Geology*, 2003, **200**, 155.
- 4
- 5 18 J. Woodhead, J. Hergt, M. Shelley, S. Eggins and R. Kemp, *Chemical Geology*, 2004, **209**, 121.
- 6
- 7 19 C. Paton, J. Woodhead, J. Hellstrom, J. Hergt, A. Greig and R. Maas, *Geochemistry Geophysics Geosystems*, 2010, **11**, 1.
- 8
- 9 20 C. Paton, J. Hellstrom, B. Paul, J. Woodhead and J. Hergt, *Journal of Analytical Atomic Spectrometry*, 2011, **26**, 2508.
- 10
- 11 21 M. Wiedenbeck, J. M. Hanchar, W. H. Peck, P. Sylvester, J. Valley, M. Whitehouse, A. Kronz, Y. Morishita, L. Nasdala, J. Fiebig, I. Franchi, J. P. Girard, R. C. Greenwood, R. Hinton, N. Kita, P. R. D. Mason, M. Norman, M. Ogasawara, P. M. Piccoli, D. Rhede, H. Satoh, B. Schulz-Dobrick, O. Skår, M. J. Spicuzza, K. Terada, A. Tindle, S. Togashi, T. Vennemann, Q. Xie and Y. F. Zheng, *Geostandards and Geoanalytical Research*, 2004, **28**, 9.
- 12
- 13
- 14 22 M. S. Brown and C. B. Arnold, in *Laser Precision Microfabrication*, ed. K. Sugioka, M. Meunier and A. Piqué, Springer Berlin Heidelberg, 2010, pp. 91.
- 15
- 16
- 17 23 X. Mao, A. Ciocan and R. Russo, *Applied spectroscopy*, 1998, **52**, 913.
- 18
- 19 24 D. Bleiner and A. Bogaerts, *Spectrochimica Acta Part B: Atomic Spectroscopy*, 2006, **61**, 421.
- 20
- 21
- 22
- 23
- 24
- 25
- 26
- 27
- 28
- 29
- 30
- 31
- 32
- 33
- 34
- 35
- 36
- 37
- A. S. Mark, L. M. Xianglei, F. Alberto, C. Wing-Tat and E. R. Richard, *Analytical Chemistry*, 1995, **67**.
- I. Horn, M. Guillong and D. Günther, *Applied Surface Science*, 2001, **182**, 91.
- H. Liu, O. V. Borisov, X. Mao, S. Shuttleworth and R. E. Russo, *Applied Spectroscopy*, 2000, **54**, 1435.
- P. Vermeesch, S. Sherlock, N. Roberts and A. Carter, *Geochimica et Cosmochimica Acta*, 2012, **79**, 140.
- P. Outridge, W. Doherty and D. Gregoire, *Spectrochimica Acta Part B: Atomic Spectroscopy*, 1997, **52**, 2093.
- A. Mank and P. Mason, *Journal of Analytical Atomic Spectrometry*, 1999, **14**, 1143.
- J. Košler, M. Wiedenbeck, R. Wirth, J. Hovorka, P. Sylvester and J. Mikova, *Journal of Analytical Atomic Spectrometry*, 2005, **20**, 402.
- W. A. Deer, ed., *Orthosilicates*, Geological Society, 1997.
- R. Ewing, *Reviews in Mineralogy and Geochemistry*, 2003, **53**.
- M. Klinger, U. Kempe, A. Pöpl, R. Böttcher and M. Trinkler, *European Journal of Mineralogy*, 2012, **24**.
- S. Jackson, H. Longrich, G. Dunning and B. Fryer, *Canadian Mineralogist*, 1992.
- E. Kooijman, J. Berndt and K. Mezger, *European Journal of Mineralogy*, 2012, **24**, 5.
- L. Nasdala, J. Hanchar, A. Kronz and M. J. Whitehouse, *Chemical Geology*, 2005, **220**.

This paper describes the source of systematic bias in U-Pb zircon dating by LA-ICP-MS

1
2
3
4
5
6
7
8
9
10
11
12
13
14
15
16
17
18
19
20
21
22
23
24
25
26
27
28
29
30
31
32
33
34
35
36
37
38
39
40
41
42
43
44
45
46
47
48
49
50
51
52
53
54
55
56
57
58
59
60

1
2
3
4
5
6
7
8
9
10
11
12
13
14
15
16
17
18
19
20
21
22
23
24
25
26
27
28
29
30
31
32
33
34
35
36
37
38
39
40
41
42
43
44
45
46
47
48
49
50
51
52
53
54
55
56
57
58
59
60

